encit 2020

ABCM
Associação Brasileira de Engenharia e Ciências Mecânicas

18th Brazilian Congress of Thermal Sciences and Engineering
November 16–20, 2020 (Online)

# ENC-2020-0085
# EXTREMUM SEEKING CONTROL APPLIED TO VORTEX SHEDDING TONAL NOISE REDUCTION IN A NACA0012 AIRFOIL

**Tarcísio Déda**
**William Wolf**
School of Mechanical Engineering, University of Campinas, Campinas, SP, Brazil
tarcisio.deda@gmail.com, wolf@fem.unicamp.br

***Abstract.*** *In the present work, the Extremum Seeking Control (ESC) technique is applied to reduce noise generated by vortex shedding in a NACA0012 airfoil. High-fidelity simulations are conducted where a suction actuator is placed at the airfoil suction side. The ESC is implemented to minimize noise generation by finding the best position for actuator placement. Different actuation setups are tested and, in some cases, flow control provides a sound pressure level reduction of -11dB without flow reattachment. For higher actuator intensities, flow reattachment occurs leading to sound pressure level reduction of -70dB.*

***Keywords:*** *flow control, extremum seeking control, active control, unstable flows*

## 1. INTRODUCTION

Control of unstable flows is sought in several engineering problems involving laminar and turbulent flows. The field of active closed-loop control finds applications, for example, in drag reduction, lift increase, heat transfer and mixing enhancement, transition and separation delay, and noise reduction. In the past, flow control has been mainly implemented in experimental setups. However, the high costs imposed by experiments may become prohibitive for flow control studies in many situations. The improvement in computational power and development of high-fidelity simulation tools enabled the simulation of complex unsteady flows together with active flow control (Gad-el Hak, 1996; Brunton and Noack, 2015). For example, the combination of computational fluid dynamics (CFD) and novel active control strategies has been shown by several authors in the literature (Ramos *et al.*, 2019; Ramirez and Wolf, 2015; Chang and Collis, 1999; Velasco *et al.*, 2017; Naghib-Lahouti and Hangan, 2010).

In the present work, we combine CFD and flow control for suppression or attenuation of airfoil noise. Unsteady flows over airfoils can generate acoustic perturbations due to a variety of physical mechanisms. For example, noise is generated when a turbulent wake impinges on the leading edge of a wind turbine or helicopter blade. On the other hand, laminar and turbulent boundary layers lead to acoustic scattering at the trailing edge, also generating what is called airfoil self-noise. In the previous cases, flow instabilities developing on the boundary layer or wake are the true sources of noise in the scattering problems. While turbulent boundary layers generate broadband noise, laminar boundary layers typically lead to the presence of tones in the noise spectrum. Ramirez and Wolf (2015) proposed an open-loop blowing actuation at the trailing edge that reduced the noise scattering by putting away the vortex shedding structures that interacted with the airfoil trailing edge. Wolf *et al.* (2015) achieved considerable noise attenuation in wind turbine blades with suction actuation. Koop *et al.* (2004) developed an active blowing configuration that was able to reduce flap side edge noise.

The previous works show the application of open-loop flow control with either passive or active strategies. Closed-loop control allows for feedback of the output to improve a desired condition, being able to stabilize an otherwise unstable system. Applying closed-loop control to a high-fidelity flow simulation is not a simple task since the system plant (the Navier-Stokes equations) is non-linear and the system may have millions (or billions) of states. One strategy that can be applied to those problems is the Extremum Seeking Control (ESC), that allows for a robust optimization of the control with respect to variations in the system operating condition. For example, Beaudoin *et al.* (2006) applied ESC in an experimental setup to find the rotational velocity of a cylinder aiming to minimize the total power loss due to drag and also the control effort. Hoeijmakers (2008) employed ESC to control the vortex shedding in a cylinder by finding the best suction/blowing intensity with two actuators in opposition. ESC is also used by Fan *et al.* (2016) to search for the best frequency of microjets to enhance mixing in the output of a round jet. Brackston *et al.* (2016) applied ESC to minimize drag forces in a bullet-shaped body by automatically seeking the optimal frequency of actuating jets produced by a speaker.

In this work, we propose the application of the ESC approach to reduce trailing-edge noise of a NACA0012 airfoil. Here, the flow is laminar and tonal noise arises due interaction of a von Kármán vortex street with the trailing edge. This model-free adaptive technique has been applied to different actuation setups. High-fidelity simulations are conducted where a suction actuator is placed at the airfoil suction side. This actuator is moved along the airfoil surface with the position determined by the controller. A cost function is computed to quantify the noise radiation and the ESC loop is configured to minimize airfoil noise generation by finding the best actuation position for a fixed actuator intensity. In the control scheme presented, benefits of closed-loop control related to plant variation robustness improve the performance of active interventions in the flow. The optimal placement of the actuator can be tracked online while accounting for sufficiently slow variations of the system variables, such as effective angle of attack and flow velocity. Results demonstrate that the ESC implementation can provide considerable noise reduction for the configurations tested.

## 2. NUMERICAL METHODOLOGY

### 2.1 Flow simulations

The present control approach is implemented in a high-fidelity flow simulation tool. The flow solver has been verified and validated in previous works (Ramos *et al.*, 2019; Ricciardi *et al.*, 2020), and it employs sixth-order compact schemes for spatial derivation, filtering and interpolation. The latter operation is required since the formulation is solved on a staggered mesh. Filtering is necessary to damp eventual high-frequency numerical waves. Direct numerical simulations are performed on 2D grids with an overlapping region, so that the inner grid with $400 \times 100$ points is solved using an implicit Beam and Warming method for time integration, while the outer one, with $400 \times 150$ points, is iterated with a low-storage third-order Runge-Kutta scheme. A detail view of the inner grid is shown by black lines in Fig. 1. A small region of the outer grid can also be seen in this figure in orange. The far-field is placed 12 chords away from the airfoil, where a buffer layer is applied together with non-reflexive boundary conditions.

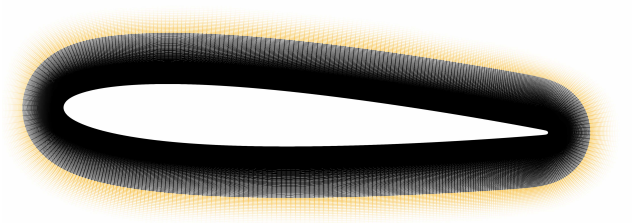

Figure 1. Detail view of the grid near the airfoil. The inner (black) and outer (orange) grids use, respectively, implicit and explicit time step methods. The inner and outer grids have $400 \times 100$ and $400 \times 150$ points, respectively.

The flow configurations investigated in this paper have Reynolds number $\mathrm{Re} = 10^4$ and Mach number $\mathrm{Ma} = 0.3$. In this flow regime, a von Kármán vortex street develops along the airfoil wake, generating tonal noise due to scattering of quadrupole sources at the trailing-edge region. The simulations are integrated using a time step $\Delta t_{\mathrm{sim}} = 4 \cdot 10^{-4}$ time units relative to free stream velocity, what guarantees stability and accuracy of solutions. The angle of attack is fixed to $3^o$.

### 2.2 Boundary layer actuation

The goal of this work is to apply actuation at the airfoil boundary layer trying to mitigate the trailing edge noise generation mechanism. The actuation setup proposed here consists of suction jet with constant momentum in the wall-normal direction. This is implemented by imposing a permeable boundary condition and the control input is given by the horizontal position of the suction jet whose value $x_c$ is computed online by the control law.

The intensity of the wall-normal momentum on each grid point $i$ at the airfoil surface is computed as $\rho_i v_i = A\, \mathcal{W}\,[2\pi(x_i - x_c)/\Delta x]$, where the window function $\mathcal{W}(x) = 0.5 + 0.5\cos(x)$, if $-\pi < x < \pi$, and $\mathcal{W}(x) = 0$ otherwise. The constant $A$ corresponds to the maximum momentum, which characterizes the actuation intensity for a given simulation. The values of $A$ used here are $4\%$ and $20\%$ of the freestream velocity. The nonzero region length $\Delta x$ is fixed to $5\%$ of the airfoil chord.

### 2.3 Extremum-seeking control

Several techniques of flow control are available in the literature (Brunton and Noack, 2015). Many of these techniques are based on linear approaches such as hydrodynamic stability analysis or resolvent analysis (Schmid and Brandt, 2014). In such cases, one usually search for a most stable frequency/wavenumber that can be disturbed to modify the flow with a maximum gain. In the present work, we apply the extremum-seeking control (ESC) approach that can be applied

directly to the flow solver without further knowledge of the dynamical system. The ESC approach can be applied to non-linear problems and, here, the Navier-Stokes equations are the plant of the system. A simplified block diagram of a default ESC control loop is presented in Fig. 2. Automatic optimal seeking is made possible by defining a cost function $J(\boldsymbol{\rho}, \boldsymbol{u}, \boldsymbol{v}, \boldsymbol{p}, x_c)$ that numerically determines how good the system is operating given $x_c$ and the flow state.

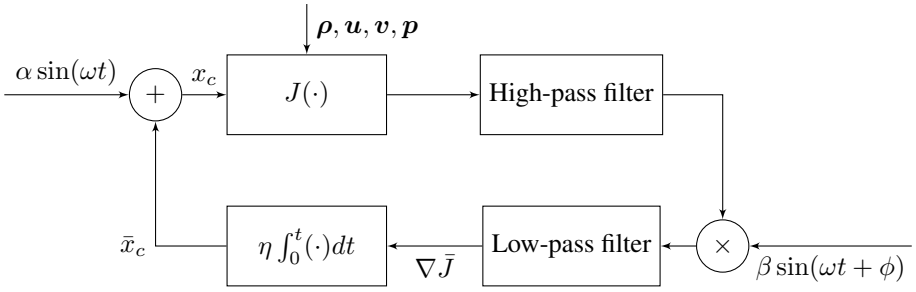


Figure 2. Simplified ESC block diagram.

Since the flow control strategy applied in the present work aims to reduce airfoil noise, the cost function is computed by directly probing pressure fluctuations. This is done by sampling the pressure $p$ at the grid node that is nearest to point $(x, y) = (0.00, 1.00)$, where the spatial coordinates are non-dimensional by the airfoil chord length. A type I Chebyshev high-pass filter is applied to $p$, providing the fluctuation $p'$. This filter is designed for a pass band ripple of -2dB and a stop band attenuation of -20dB. The cutoff frequency is fixed to 40% of the measured acoustic signal frequency (computed for an oscillation period of 0.3675 time units relative to free stream velocity) without active control, and the pass/stop band frequency ratio set to 300%. All discrete components of the control loop, including filters, cost function evaluation and sampling, are set with a discretization time $\Delta t_{\text{control}} = 80 \Delta t_{\text{sim}}$.

The cost function is then calculated according to

$$J_k = \left( \sum_{i=0}^{n-1} {p'}_{k-i}^{\,2} \right)^{\sigma} , \tag{1}$$

where ${p'}_k$ is the pressure fluctuation at control iteration $k$, $n$ is the number of iterations used in signal power estimation and $\sigma$ is set to tighten the difference between high and low values assumed by the cost function. Next, high-pass filtering is applied to the calculated cost as indicated in Fig. 2. The filtered signal represents the variational behavior of the cost function to a sinusoidal perturbation $\alpha \sin(\omega t)$. The oscillating response is then multiplied by another sinusoidal signal $\beta \sin(\omega t + \phi)$, where $\phi$ is a phase correction constant that, in the present work, is always computed as the phase added by the linear high-pass filter at frequency $\omega$. This high-pass filter is also designed as Chebyshev type I.

The multiplication result is then low-pass filtered, which results in a signal $\nabla \bar{J}$ that is approximately proportional to the cost function gradient, although it carries delays from the low-pass filtering. This filter is also a Chebyshev type I in the present work. The partial control input $\bar{x}_c$ is then estimated through the law $\dot{\bar{x}}_c = \eta \nabla \bar{J}$. The parameter $\eta$ must be set to a negative constant for the minimization problem. The present work implements the numerical integration via the trapezoidal rule. The control parameters for each subsystem are presented in the results section.

## 3. RESULTS

This section presents simulation results for a NACA0012 airfoil immersed in a $\mathrm{Ma} = 0.3$ flow. The chord-based Reynolds number is set as $\mathrm{Re} = 10^4$ and, therefore, a laminar flow regime develops vortex shedding. The flow unsteadiness leads to subsequent tonal noise which should be reduced by the ESC approach. In this work, four cases are analyzed as summarized in Table (1), which presents the parameters chosen for each case. Table (2) shows specific parameters used in filters designs and the ESC implementation depicted in Fig. 2. As can be observed from the tables, actuation is tested for two amplitudes $A$ which are a percentage of the sound speed. The actuators start at different positions $x_c$ either near the leading or trailing edge of the airfoil.

Table 1. Parameters used for each simulation.

| Simulation | $A$ | $x_c(t=0)$ | $\alpha = \beta$ | $\sigma$ | $n$ | $T = 2\pi/\omega$ | $\eta$ |
|---|---|---|---|---|---|---|---|
| 1 | -0.060 | 0.15 | 0.01 | 0.20 | 20 | 40.0 | -50.0 |
| 2 | -0.060 | 0.92 | 0.01 | 0.20 | 20 | 40.0 | -50.0 |
| 3 | -0.012 | 0.20 | 0.01 | 0.20 | 20 | 100.0 | -200.0 |
| 4 | -0.012 | 0.82 | 0.01 | 0.20 | 20 | 100.0 | -200.0 |

Table 2. Filter specifications for each simulation.

| Sim | HP cutoff frequency | HP $\omega_p/\omega_s$ ratio | LP cutoff frequency | HP $\omega_s/\omega_p$ ratio |
|---|---|---|---|---|
| 1 | 0.3·$\omega$ | 3.0 | 0.4·$\omega$ | 3.0 |
| 2 | 0.3·$\omega$ | 3.0 | 0.4·$\omega$ | 3.0 |
| 3 | 1.0·$\omega$ | 3.0 | 0.8·$\omega$ | 3.0 |
| 4 | 1.0·$\omega$ | 3.0 | 0.8·$\omega$ | 3.0 |

Results show that the closed loop system is able to minimize the cost functions presented in Fig. 3 for simulations 1 (left) and 3 (right). These simulations start with the flow actuation close to the leading edge but with different actuation intensities and frequencies. One can observe that the minimization paths are different; while simulation 1 reaches a minimum at around 400 time units, simulation 3 does so in 1500 time units. In the cases for which $A$ is higher, flow reattachment occurs eliminating vortex shedding and, thus, noise generation. Hence, the cost function reaches lower values for these cases.

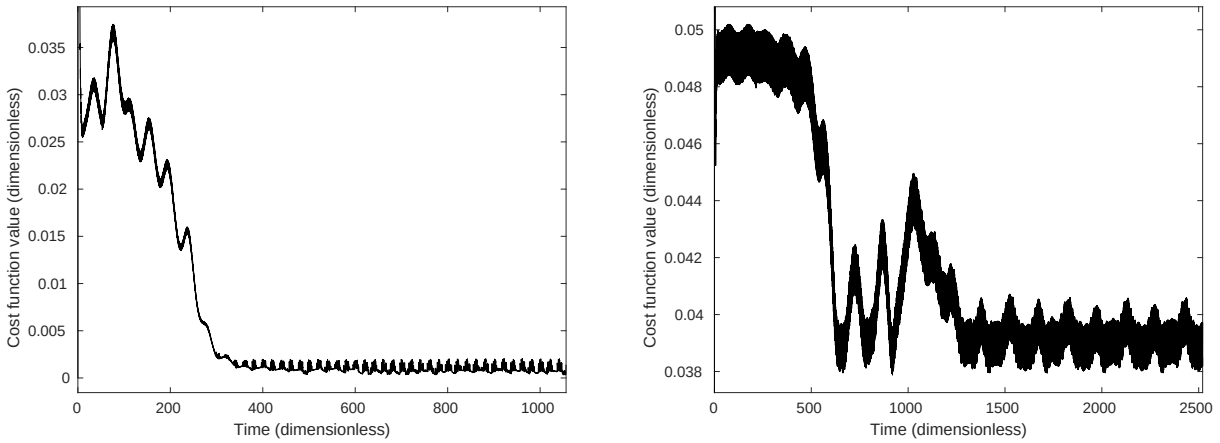


Figure 3. Cost function for simulations 1 (left) and 3 (right). The cost function signal is reduced over time and it is possible to verify that, in simulation 1, which has stronger actuation intensity $A$, the cost function reaches lower values than for simulation 3. This is a result of flow reattachment that occurs for the first case, eliminating the noise generation mechanism which is the trailing edge vortex shedding.

When the higher intensity is applied, there is a region of actuation on the airfoil suction side at which flow reattachment takes place. The boundaries of this region can be observed in Fig. 4 which shows the center of the actuation $x_c$ and its integrated value $\bar{x}_c$ during the minimization of the cost function. These boundaries can be found when the solution is converged. By setting the initial guess for $x_c$ near the leading or the trailing edges, the flow reattaches at different positions and any region in the range $0.22 < \bar{x}_c < 0.65$ can provide steady flows. When reattachment occurs, the gradient of the cost function reduces abruptly, and $x_c$ varies only due to residual pressure fluctuations reaching the farfield due to the actuator movement. The overshoots observed in both cases are a result of fast transients in the high-pass filter.

Figure 5 illustrates the actuator position for the simulations with $A = 0.012$. Since there is no reattachment for this actuation intensity, noise generated due to vortex shedding is attenuated, but not completely mitigated. The controller can then find an optimal position instead of a plateau, which can be seen in Fig. 5 at $x_c \approx 0.4$. The optimal position of actuation is found independently of the starting position. For these simulations, the integrated actuator position presents an oscillatory behavior which could be due to the large integrator gain.

To quantify the improvement in noise reduction achieved by the ESC, the amplitude of pressure fluctuations are compared. When there is no actuation, the fluctuation amplitude $p'_0 \approx 3.5 \cdot 10^{-4}$ is measured. With $A = 0.012$, the fluctuation is reduced to $p'_1 \approx 9.8 \cdot 10^{-5}$, which is equivalent to a sound pressure level reduction of $20\log_{10}(p'_1/p'_0) \approx -11.0$dB. Flow control with a stronger actuation of $A = 0.06$ reduces the amplitude $p'_2$ to less than $10^{-7}$, an attenuation of at least $20\log_{10}(p'_2/p'_0) \approx -70$dB. In this case, the measured noise comes from the actuator movement, which occurs due only to the harmonic perturbation $\alpha\sin(\omega t)$ since vortex shedding is completely mitigated as shown in Fig. (6).

Although results also showed that drag, lift and pitching moment characteristics are improved by the present flow actuation, further data processing will be conducted in future work to quantify these benefits. Further studies also include different actuation setups such as fixed position and variable amplitude, simulations at higher Reynolds numbers (Ricciardi *et al.*, 2020), slope seeking compensation for cost functions with plateaus (Benard *et al.*, 2010) and application of ESC and slope seeking techniques to close the loop in a trailing edge blowing configuration (Ramirez and Wolf, 2015).

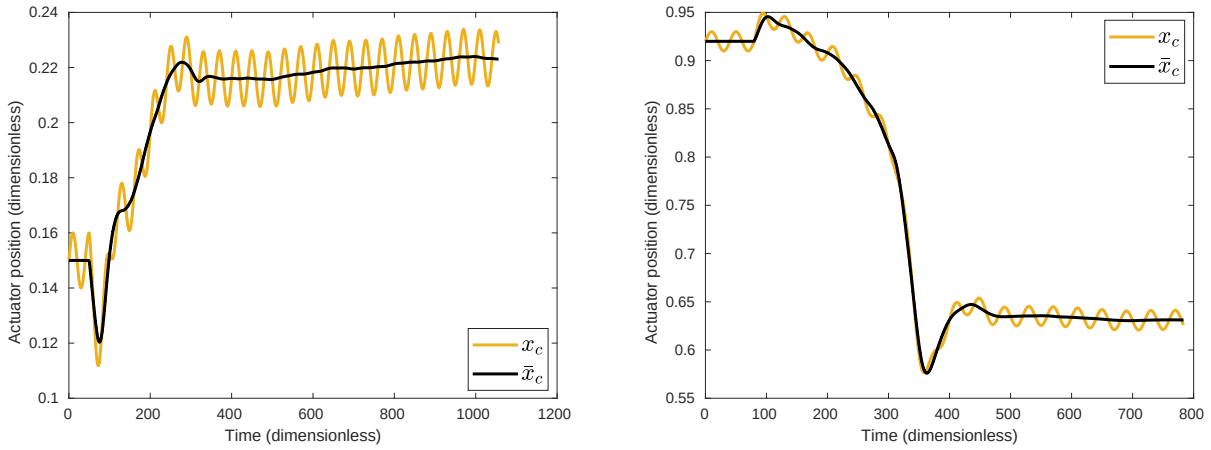


Figure 4. Actuation position $x_c$ and its integrated output $\bar{x}_c$ for simulations with $A = 0.060$. In simulation 1 (left) reattachment occurs at $t \approx 300$ while, in simulation 2, reattachment is reached at $t \approx 350$. For both cases, the overshoots indicate the instant of reattachment.

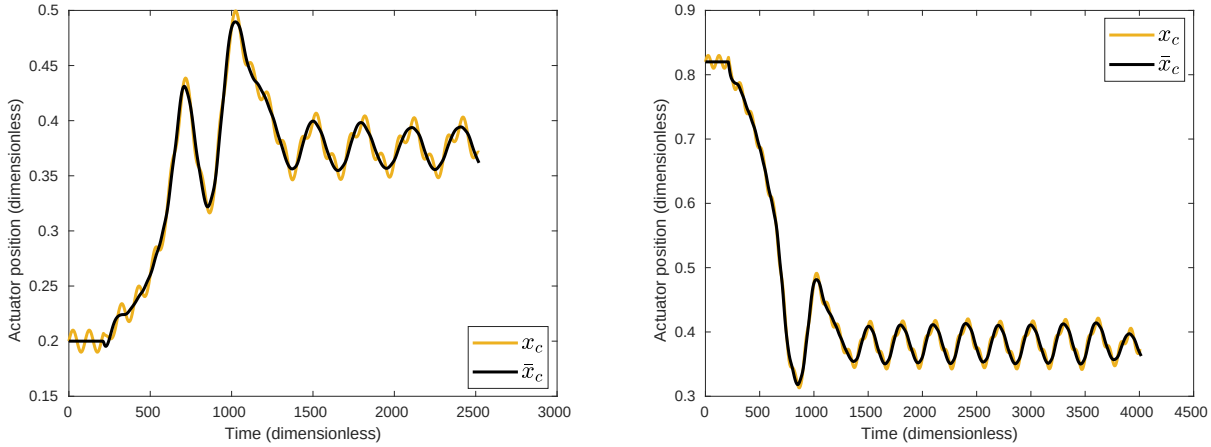


Figure 5. Actuation position $x_c$ and its integrated output $\bar{x_c}$ for simulations 3 (left) and 4 (right) with $A = 0.012$. The oscillatory behavior of $\bar{x_c}$ could be related to the large integrator gain.

Figure 6. Contour lines of vorticity without actuation (top) and with a reattached flow (bottom) obtained from simulation 1, with $x_c \approx 0.22$. Black lines indicate positive vorticity of 0.3 and 0.4, while yellow lines correspond to negative values -0.3 and -0.4. On flow reattachment, dynamic shedding of cohere structures responsible for noise generation cease.

## 4. CONCLUSIONS

Active flow control is applied to an unsteady flow aiming to reduce the farfield noise radiation. For the present flow configuration, an airfoil is immersed in a compressible flow and vortex shedding at the trailing edge is responsible for noise generation. Acoustic scattering is an efficient mechanism of noise radiation and a tonal component is observed at the vortex shedding frequency. In order to mitigate noise radiation to the farfield, the extremum seeking control (ESC)

approach is implemented in a high-fidelity flow simulation tool for different setups including different intensities and frequencies of actuation. We observe that, for a lower actuation setup, the sound pressure level is reduced by $-11$dB when the ESC finds the optimal actuation position. Independently of the initial position, this optimal position is found by the ESC. For a higher actuation intensity, the ESC can reattach the flow leading to a noise reduction by $\approx -70$ dB. In these cases, the residual noise is due only to the motion of the actuator, and an optimal region of control is found since the flow reattaches for an actuation position between $22\%$ and $65\%$ of the airfoil chord.

## 5. ACKNOWLEDGEMENTS

The authors acknowledge the financial support received from Fundação de Amparo à Pesquisa do Estado de Sâo Paulo, FAPESP, under Grant No. 2013/08293-7. The first author is supported by the FAPESP PhD scholarship 2019/19179-7, which is also acknowledged. The computational resources used in this work were provided by CENAPAD-SP through Project 551, and by SINAPAD via the Santos Dumont cluster.

## 6. REFERENCES

Beaudoin, J.F., Cadot, O., Aider, J.L. and Wesfreid, J.E., 2006. "Bluff-body drag reduction by extremum-seeking control". *Journal of fluids and structures*, Vol. 22, No. 6-7, pp. 973–978.

Benard, N., Moreau, E., Griffin, J. and Cattafesta III, L.N., 2010. "Slope seeking for autonomous lift improvement by plasma surface discharge". *Experiments in fluids*, Vol. 48, No. 5, pp. 791–808.

Brackston, R.D., Wynn, A. and Morrison, J.F., 2016. "Extremum seeking to control the amplitude and frequency of a pulsed jet for bluff body drag reduction". *Experiments in Fluids*, Vol. 57, No. 10, p. 159.

Brunton, S.L. and Noack, B.R., 2015. "Closed-loop turbulence control: progress and challenges". *Applied Mechanics Reviews*, Vol. 67, No. 5, p. 050801.

Chang, Y. and Collis, S.S., 1999. "Active control of turbulent channel flows based on large eddy simulation". *ASME Paper No. FEDSM-99*, Vol. 6929, pp. 1–8.

Fan, D., Wu, Z., Cao, H., Yang, H. and Zhou, Y., 2016. "A novel extremum seeking scheme for closed-loop jet control".

Gad-el Hak, M., 1996. "Modern developments in flow control". *Applied Mechanics Reviews*, Vol. 49, No. 7, pp. 365–379.

Hoeijmakers, P., 2008. "Implementation of an extremum seeking controller for vortex shedding attenuation in a 2d cfd code". *TU Eindhoven*.

Koop, L., Ehrenfried, K. and Dillmann, A., 2004. "Reduction of flap side-edge noise: Passive and active flow control". In *10th AIAA/CEAS Aeroacoustics Conference*. p. 2803.

Naghib-Lahouti, A. and Hangan, H., 2010. "Active flow control for reduction of fluctuating aerodynamic forces of a blunt trailing edge profiled body". *International journal of heat and fluid flow*, Vol. 31, No. 6, pp. 1096–1106.

Ramirez, W.A. and Wolf, W., 2015. "The effects of suction and blowing on tonal noise generation by blunt trailing edges". In *21st AIAA/CEAS Aeroacoustics Conference*. p. 2364.

Ramos, B.L., Wolf, W.R., Yeh, C.A. and Taira, K., 2019. "Active flow control for drag reduction of a plunging airfoil under deep dynamic stall". *Physical Review Fluids*, Vol. 4, No. 7, p. 074603.

Ricciardi, T.R., Arias-Ramirez, W. and Wolf, W.R., 2020. "On secondary tones arising in trailing-edge noise at moderate reynolds numbers". *European Journal of Mechanics-B/Fluids*, Vol. 79, pp. 54–66.

Schmid, P.J. and Brandt, L., 2014. "Analysis of fluid systems: Stability, receptivity, sensitivity". *Applied Mechanics Reviews*, Vol. 66, No. 2.

Velasco, D., Mejia, O.L. and Laín, S., 2017. "Numerical simulations of active flow control with synthetic jets in a darrieus turbine". *Renewable Energy*, Vol. 113, pp. 129–140.

Wolf, A., Lutz, T., Würz, W., Krämer, E., Stalnov, O. and Seifert, A., 2015. "Trailing edge noise reduction of wind turbine blades by active flow control". *Wind Energy*, Vol. 18, No. 5, pp. 909–923.

## 7. RESPONSIBILITY NOTICE

The authors are solely responsible for the printed material included in this paper.